Research Article

In-silico identification of novel inhibitors for human Aurora kinase B form the ZINC database using molecular docking-based virtual screening

Ashraf Ahmed Ali Abdusalam[1]

1 *Department of Pharmaceutical Sciences, Faculty of Health Sciences, Sirte University, Sirte, Libya*

Corresponding author: Ashraf A. A. Abdusalam (aalmansory@su.edu.ly)

Citation: Abdusalam AAA (2022) *In-silico* identification of novel inhibitors for human Aurora kinase B form the ZINC database using molecular docking-based virtual screening. Research Results in Pharmacology 8(4): 89–99. https://doi.org/10.3897/rrpharmacology.8.82977

Abstract

Introduction: Aurora kinase enzymes play critical functions in mammals. Aurora kinases are mitotic regulators that are involved in a variety of processes during cell division. The overexpression of these enzymes is associated with tumour formation and is symptomatic of clinical circumstances in cancer patients who have been diagnosed.

Materials and methods: The current study reports an *in-silico* virtual screening (VS) and molecular docking analysis of 2500 compounds retrieved from the ZINC database and five current clinical trial compounds against Aurora Kinase B using AutoDock Vina to identify potential inhibitors.

Results and discussion: The top six compounds that resulted from the screening were ZINC00190959, ZINC07889110, ZINC0088285, ZINC01404326, ZINC00882846 and ZINC08813187, which showed lower free energy of binding (FEB) against the target protein binding pocket. The FEB were as follows: -11.92, -11.85, -11.46, -11.33, -11.21 and -11.1 kcal/mol, using AutoDock, and -11.7, -11.5, -11.2, -11.0, -10.8 and -10.6 kcal/mol for AutoDock Vina, respectively. These findings were superior to those obtained with the co-crystallized ligand VX-680, with a -7.5 kcal/mol and the current clinical trial drug. Finally, using a VS and molecular docking approach, novel Aurora kinase B inhibitors were effectively identified from the ZINC database fulfilling the Lipinski rule of five with low FEB and functional molecular interactions with the target protein.

Conclusion: The findings suggest that the six compounds could be used as a potential agent for cancer treatments.

Graphical abstract
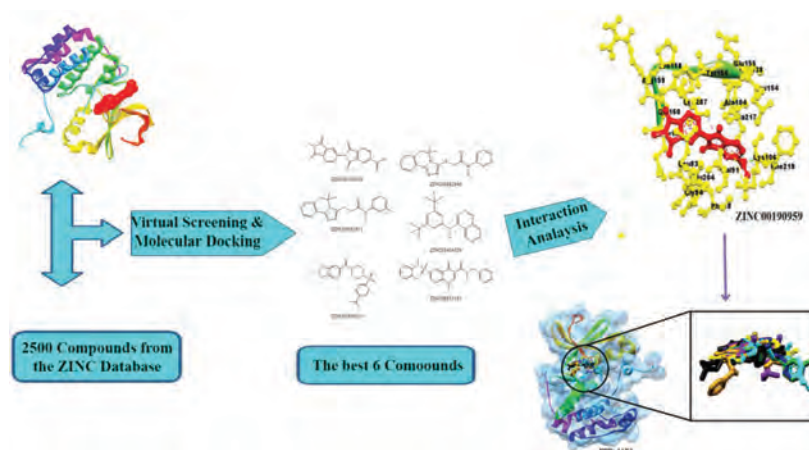
Keywords

Introduction

Cancer is a complex disease that can be recognized by its hallmark symptoms, which include uncontrolled cell division and proliferation caused by the blocking of the normally occurring process of cell division (Rashid et al. 2009; Bourzikat et al. 2022). It is regarded as one of the most lethal diseases threatening our lives. In addition, the cancer mortality rate continues to rise, and it is projected that it will surpass the cardiovascular disease mortality rate in the near future (Al-Warhi et al. 2020). According to the current biological theories of cancer, all malignancies are the consequence of a combination of genetic and environmental factors, which indicates that a variety of external influences and internal genetic alterations can cause cancer in people. It is possible to prevent the disruption of cellular signaling and defensive pathways by preventing all carcinogenic exposures from outside the body. The prevention of carcinogenic exposures is still a significant priority (Mbemi et al. 2020). It is now known that both alterations are present in cancer cells and in normal cells many years before cancer develops. Environmental influences are connected with distinct patterns of change. The buildup is linked to cancer risk and can be used to diagnose cancer risk. With or without the proliferation of physiological patches of clonal cells, tissue with accumulated abnormalities is known as a "field for cancerization" (cancerization field) (Yamashita et al. 2018; Takeshima and Ushijima 2019). In addition, the difference in mitotic regulation, which requires well-coordinated cellular activities to ensure cell division and genomic stability, led to genetic instability, a distinguishing hallmark of many human malignancies (Negrini et al. 2010; Shen 2011). When the regulation of mitosis is disrupted, centrosome duplication, chromosomal segregation, and cytokinesis are disrupted, resulting in cell transformations (Failes et al. 2012). Aneuploidy has been regarded as a hallmark of cancers for a very long time. 90% of solid tumours exhibit some degree of aneuploidy, and the vast majority of human malignancies, regardless of their origin, exhibit chromosomal instability (Kuang and Li 2022). Thus, blocking amplified or overexpressed enzymes involved in mitotic cell division to manage these altered pathways is a treatment strategy for various cancers (Chohan et al. 2018).

The well-established mitotic protein kinases of the cell cycle show increased expression levels in a variety of malignant behaviours associated with cancer. Due to their aggressive nature, they are of great interest in cancer therapy targeting these kinases (Welburn and Jeyaprakash 2018; Fulcher and Sapkota 2020). The Aurora kinase family is a set of mitotic kinases in the cell cycle that is critical for regulating various signalling pathways essential for accurate cell division and genetic stability (Brognard and Hunter 2011; Chan et al. 2012; Lin et al. 2014). The three homologous serine/threonine kinases (Aurora A, Aurora B, and Aurora C) are members of a small family of three serine/threonine kinases that have crucial roles in mammals, particularly in cell cycle regulation (Carmena and Earnshaw 2003). At the level of amino acids, the catalytic domains of all three Aurora kinases – Aurora A, Aurora B, and Aurora C – are identically sequenced to each other to a degree that is 70% similar. The other domains, on the other hand, are highly diverse. Therefore, whereas all Aurora kinases show significant similarities in their sequences, they all have distinct subcellular localizations and functions (Willems et al. 2018; Ahmed et al. 2021). The three enzymes Aurora kinase (A, B, and C) have been identified as candidates for use as potential targets to discover new and more effective cancer treatments. Aurora B kinase B is of particular interest, which was activated by the phosphorylation of itself and INCENP (Inner Centromere Protein). Aurora B is a chromosomal passenger protein that, depending on the cell cycle phase in which it is found, can be found in various sites within the mitotic apparatus (Willems et al. 2018). Patients who have already been diagnosed with the malignant disease may have a worsening clinical status due to the overexpression of Aurora enzymes, which has been linked to various types of tumour processes (Bhullar et al. 2018). Human Aurora B's structure was previously determined in complex with INCENP and VX-680 (Elkins et al. 2012). Drug development and production are challenging because drug discovery is a time-consuming and resource-intensive process. The processes of drug discovery, lead optimization, drug design, and development have been accelerated with computers and information technology (Velmurugan et al. 2020).

Because of its ability to reduce the time and resources needed to discover new drugs, in-silico technology has emerged as an indispensable tool in the modern pharmaceutical industry. As a result of developments in computer algorithms and the accumulated knowledge databases over time, computational prediction tools have recently been incorporated into every stage of the drug discovery process (Shaker et al. 2021). It has been demonstrated that computational methods for drug discovery can successfully be used to design and find therapeutic molecules for the treatment of various diseases, including cancer (Cordeiro and Speck-Planche 2012), bacteria (Dai et al. 2018; Duan et al. 2019) and viral diabetes (Balamurugan et al. 2012). In 1997, the term "virtual screening" or "virtual ligand screening" was first used in the literature (Horvath 1997); VS is a computational approach used to search

libraries of small molecules for chemical compounds that are likely to bind to one or more therapeutic targets early in the drug development process (Abagyan and Totrov 2001; Shoichet 2004; Phatak et al. 2009; Cavasotto et al. 2018). In general, virtual screening computations coupled with interactive data analysis will yield a list of compounds that require experimental validation (Martin and Jansen 2020; Stumpfe and Bajorath 2020). ZINC (ZINC Is Not Commercial) is a free-to-use database and toolset initially intended to facilitate the rapid availability of compounds for virtual screening (Irwin and Shoichet 2005). However, the library is increasingly being widely used for virtual screenings (Carlsson et al. 2010; Irwin et al. 2012; Abdalsalam 2017; Abdusalam and Vikneswaran 2020), ligand discovery (Liu et al. 2007; Carlsson et al. 2010; Irwin et al. 2012; Abdalsalam 2017; Abdusalam and Vikneswaran 2020), pharmacophore screens (Zoete et al. 2011), and force field development (Mysinger and Shoichet 2010). Additionally, the database provides information about the compounds' chemical and physical properties, such as their log P, the number of hydrogen bond acceptors, donors, molecular weight, and the type of bonds (Irwin et al. 2012). The aim of the current study was to use virtual screening followed by molecular docking analysis to identify, discover and evaluate novel Aurora kinases B inhibitors retrieved from the ZINC database and compare the results with FDA-approved drugs, where the identified potential compounds could be used as novel anticancer drugs.

Materials and methods

Preparation of protein

The crystal structure of Human Aurora B Kinase in complex with VX-680 (PDB: 4AF3) has a resolution of 2.75 A (Elkins et al. 2012) Fig. 1 was obtained from Protein Data Bank (www.rcsb.org); the crystal structure consists of the chain (A). The protein was edited with AutoDockTools (ADT) by removing unwanted water molecules and adding hydrogen atoms.

Ligand screening from ZINC database

The three-dimensional structures of 2000 ligand molecules were obtained in mol2 format from the ZINC database (Irwin and Shoichet 2005), and then converted to pdbqt using raccoon (Forli et al. 2016) to be used for VS with AutoDock Vina. Molecular properties such as calculated log P, molecular weight, number of hydrogen-bond acceptors, number of hydrogen-bond donors and number of rotatable bonds; these data were derived and calculated from the ZINC database; the purpose was to assess the likelihood of the molecules to have drug-like properties.

Virtual screening and molecular docking

Virtual screening was performed using AutoDock Vina, followed by molecular docking using AutoDock 4.2. along with AutoDockTools (ADT) (Morris et al. 1998) for the top six compounds. A grid box with dimensional 60, 60, and 60 for x, y, z coordinates in Å was positioned at the enzyme's binding site centre. By using raccoon software, the ligands were converted from mol2 to pdbqt. The Confi.txt file prepared with (ADT) contains all of the parameters needed to do the virtual screening. One hundred independent runs for the top six compounds were carried out for each docking experiment; other settings were considered defaults.

Results and discussion

Control docking

Before conducting molecular docking using AutoDock Vina, the control docking procedure was performed by extracting the coordinated ligand VX-680 from the Human Aurora Kinase B crystallographic structure (PDB:
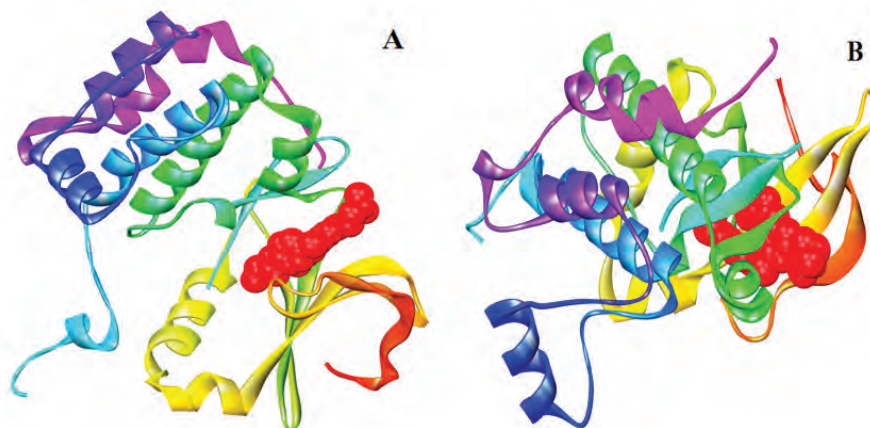

Figure 1. Schematic representation of the 3D structure of Human Aurora B Kinase (4AF3) coordinated with VX-680 red color in CPK format.

4AF3) and then re-docked into the same location of the binding pocket. The results showed that the binding pose conformation of the re-docked ligand was similar to the crystallographic pose and considered acceptable with the RMSD value = 0.78 Å, Fig. 2, demonstrating that docking software parameters used can be amenable to this system. The root mean square deviation (RMSD) value (0.78 Å) indicate the reliability of the docking protocol used, where the RMSD 2.0 Å was considered as the threshold of reliability (Bourne et al. 2003).
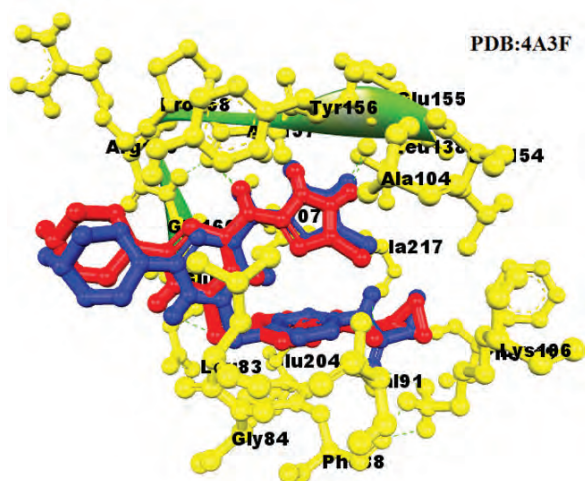

Figure 2. Superimposition between the docked conformation (red) and crystallographic VX-680 (blue) with the (4AF3).

Firstly, virtual screening using AutoDock Vina was performed for 500 compounds obtained from the ZINC database. To exclude the compounds that cannot be an effective drug, Lipinski's rule of five was applied to assess the drug-likeness of compounds based on their molecular properties (Lipinski 2004). The molecular properties obtained from the ZINC database website, such as H-bond acceptors, H-bond donors, molecular weight, log P, and a number of rotatable bonds. The compounds that violate one of the Lipinski's rule of five were excluded Based on the results of AutoDock Vina scores, as shown in Fig. 3, six candidates were selected. Those compounds exhibited the lowest binding energy; therefore, they were used further for the docking calculation. Table 1 lists the molecular properties of the six compounds that were chosen.

The obtained results of VS revealed that the range of the lowest binding energy was from −4.3 to −9.5 kcal/mol. The lowest value of binding energy of the involved

Table 1. Molecular properties of the 6 compounds obtained from ZINC Database

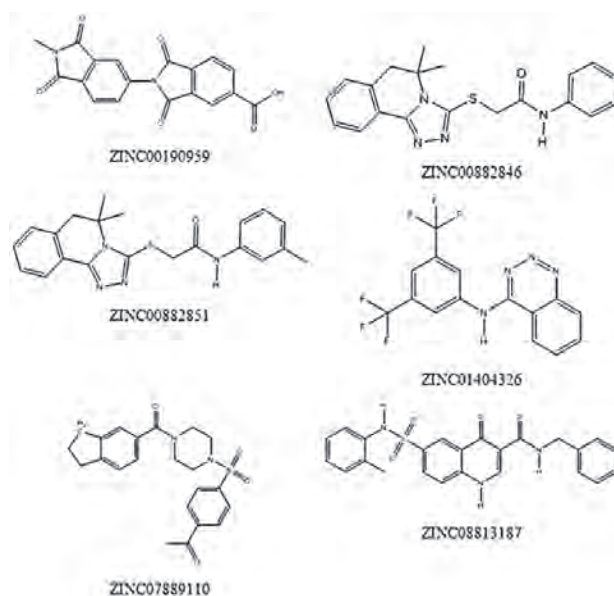| NO	Compounds	xlogP	H-bond acceptors	H-bond donors	Rotatable bonds	Molecular weight (g/mol)
1	ZINC00190959	1.411	6	0	2	350.286
2	ZINC07889110	2.525	4	0	4	412.511
3	ZINC00882851	4.276	4	1	5	378.501
4	ZINC01404326	4.806	4	1	2	358.254
5	ZINC00882846	3.967	5	1	4	364.474
6	ZINC08813187	3.567	4	3	6	447.516

Figure 3. Structure of the 6 candidates (1) ZINC00190959), (2) ZINC07889110), (3) ZINC00882851, (4) ZINC01404326, (5) ZINC00882846), (6) ZINC08813187.

protein-ligand complex is usually considered characteristic of a potential inhibitor (Fodero et al. 2004); therefore, the top six compounds that were considered potential in this study showed the lowest binding energy. The selected compounds – ZINC00190959, ZINC07889110, ZINC00882851, ZINC01404326, ZINC00882846 and ZINC08813187 – exhibited binding energy -11.92, -11.85, -11.46, -11.33, -11.21 and -11.10 kcal/mol using AutoDock 4.2 and -11.7, -11.5, -11.2, -11.0, -10.8 and -10.6 kcal/mol using AutoDock Vina, respectively (Table 2).

The results obtained with AutoDock were grouped into

Table 2. Binding energy values of the 6 compounds obtained from ZINC Database

NO	Compounds	AutoDock 4.2 (kcal/mol)	AutoDockVina (kcal/mol)
1	ZINC00190959	-11.92	-11.7
2	ZINC07889110	-11.85	-11.5
3	ZINC00882851	-11.46	-11.2
4	ZINC01404326	-11.33	-11.0
5	ZINC00882846	-11.21	-10.8
6	ZINC08813187	-11.10	-10.6

clusters of solutions (Smith et al. 2004), that shared a similar pose and free energy of binding (Table 3). It is widely accepted that protein-ligand docking is a computational technique for predicting the conformation and orientation (pose) of the ligands used when they are bound to a given protein (Taylor et al. 2002; Sousa et al. 2013; Lohning et al. 2017). For ZINC00190959, the results indicated that 98 poses (the largest cluster of 100 poses) adopted a favorable conformation. ZINC07889110 exhibited this pose 30 times, whereas ZINC00882851 exhibited this pose 19 times out of 100, the lowest among the other compounds. ZINC01404326 adopted this pose 98 times out of 100, similar to compound ZINC00190959, ZINC00882846 ad-

opted this pose 55 times out of 100, and finally, compound ZINC08813187 adopted this pose 22 times out of 100. Table 3 shows the optimal docking solution (lowest binding energy) obtained using AutoDock for each GA run, as well as cluster analysis. These results displayed the number of AutoDock clusters, the cluster rank of selected docked structures, the docked free energy range, and the docked free energy of selected docked structures. As a result, the docking mode with the lowest docked energy was the only factor in making the final selection from these clusters.

Table 3. Relative cluster rank and docked free energies of selected docking modes

NO	Compounds	Number of AutoDock cluster	Cluster rank of selected docked structure	Docked free energy range of docked structures	Docked free energy of selected docked structure
1	ZINC00190959	98 (100)	1	-11.92 to -11.11	-11.92
2	ZINC07889110	30 (100)	1	-11.85 to -10.98	-11.85
3	ZINC00882851	19 (100)	3	-11.46 to -10.11	-11.46
4	ZINC01404326	98 (100)	1	-11.33 to -10.42	-11.33
5	ZINC00882846	55 (100)	1	-11.21 to -10.34	-11.21
6	ZINC08813187	22 (100)	4	-11.10 to -10.01	-11.10

The selected six compounds were completely enveloped by the essential amino acids in the binding pocket (Fig. 4).

These compounds were examined for their location in the binding pocket. The analysis results of the interactions between the compounds and amino acids displayed that
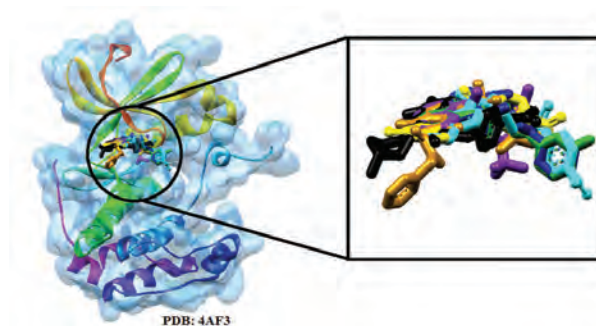

Figure 4. Enfolding of the 6 compounds in the active site pocket (1) ZINC00190959 Yellow, (2) ZINC07889110 Cyano, (3) ZINC00882851 Green, (4) ZINC01404326 Purple, (5) ZINC00882846 Blue, (6) ZINC08813187 Orange and VX-680 Black.

all of the selected compounds positioned deeply in the active pocket of the target protein with similar strength, meaning that this specific part of the protein could be attacked. Consequently, they ovalently bound by the essential active site amino acids residues of 4AF3.

The docked molecules' interactions with Human Aurora B Kinase were manually investigated utilizing AutoDockTool, LigPlot AutoDockTool, LigPlot (Laskowski and Swindells 2011) and a discovery studio visualizer. Figs 5, 6 illustrate the various interactions between the potential compounds and the essential amino acid residues that form the binding pocket. The formed interactions are electrostatic, van der Waals interactions,
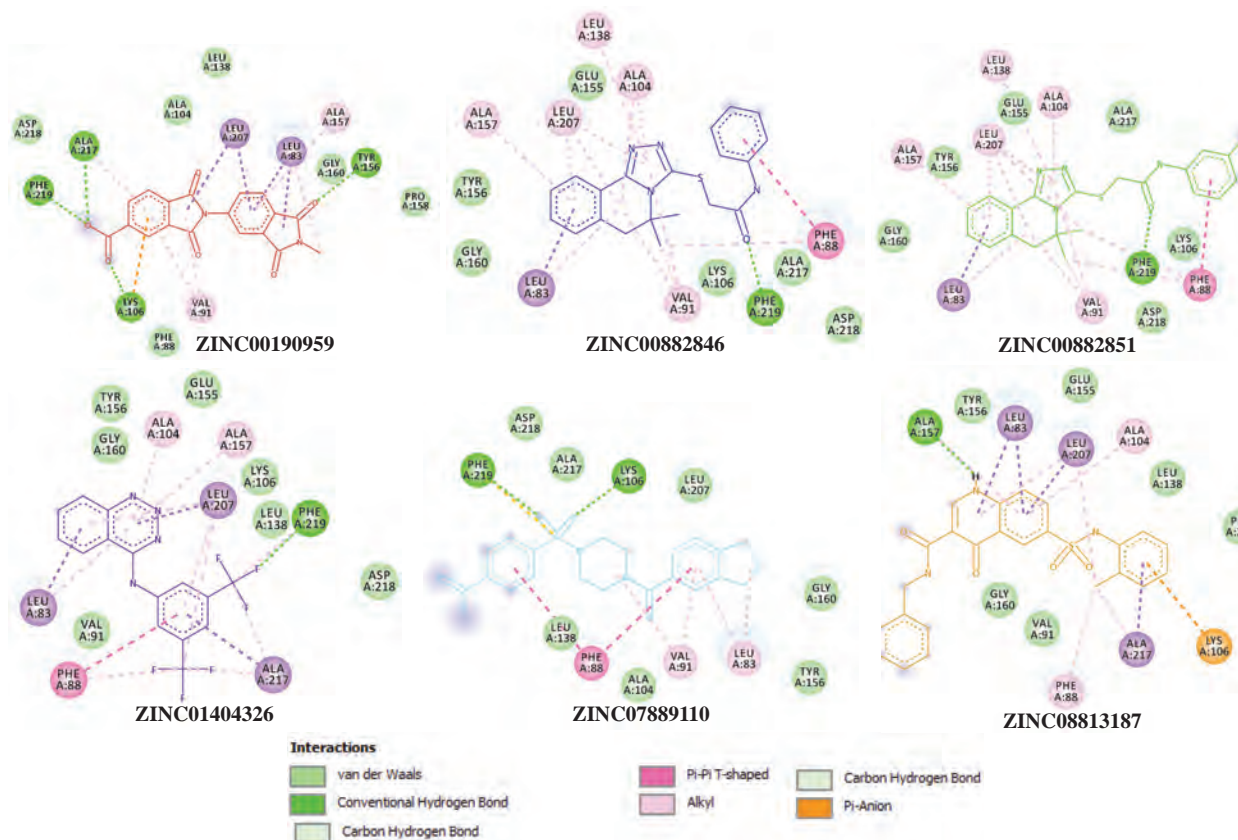

Figure 5. Binding modes in 2D of the 6 compounds: (1) ZINC00190959, (2) ZINC07889110, (3) ZINC00882851, (4) ZINC01404326, (5) ZINC00882846, (6) ZINC08813187.
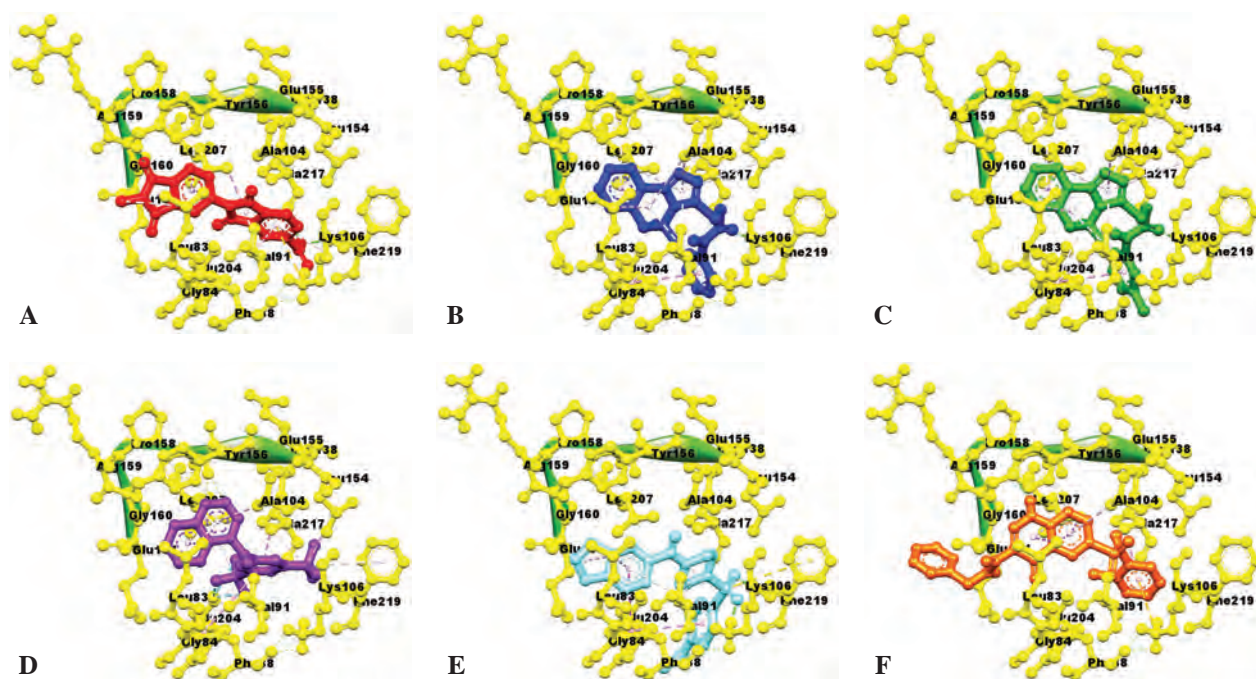
Figure 6. Binding modes in 3D of the 6 compounds: (**A**) ZINC00190959, (**B**) ZINC07889110, (**C**) ZINC00882851, (**D**)ZINC01404326, (**E**) ZINC00882846, (**F**) ZINC08813187.

H-bonding, Pi-sulfur, Pi-alkyl, Pi-Pi T-shaped and hydrophobic interactions.

The potential compound ZINC00190959 was the best among the six selected, which displayed the lowest FEB -11.7 kcal/mol, followed by compounds ZINC07889110, ZINC00882851, ZINC01404326, ZINC00882846 and ZINC08813187 with FEB of -11.5, -11.2, -11.0, -10.8 and -10.6 kcal/mol, respectively. Compound ZINC00190959 displayed four hydrogen bonds formed between amino acids Phe219, Ala217, Try156, Lys106 and four oxygen atom O_2. The docking results revealed a variety of possible interactions between the amino acids in the binding pocket. Van der Waals interaction was formed between the amino acids Phe88, Ala218, Ala104, Leu138, Gly160, Pro158 and the carbon atoms C-1, C-2, C-3, C-5, C-10, of the compound, respectively. Amino acid Leu207, Leu83 showed Pi-Sigma interaction with one benzene ring and two furan rings. Likewise, the amino acid Lys106 exhibited Pi-cation. The hydrophobic interactions were displayed with amino acids Leu154, Val91, Gly160, Leu83, Leu207, Ohe88, Ala217 at the binding pocket (Table 4 and Figs 5, 7).

Compound ZINC07889110 was found to show two H-bonds with Lys106, Phe219 and two-atom oxygen. The compound displayed van der Waals interaction between the amino acid residues Leu138, Ala104, Tyr156, Gly160, Leu207, Ala217, Asp218 and the carbon atoms C-1, C-2, C-6, C-8, C-10, C-12, C-15, C-17 of the compound. In contrast, hydrophobic interactions were shown between Glu204, Phe88, Gly84, Val91, Leu83, Glu160, Ala217, Asp218 and different atoms atthe binding pocket. Another interaction Pi-Alky between Leu83, Val91 and benzene and furan rings; likewise, two Pi-Pi-T-shaped were formed between two benzene rings. Also,

the compound exhibited one Pi-Sulfur between Phe219 and oxygen atom (Table 4 and Figs 5, 7). Compound ZINC00882851 formed one H-bond between Phe219 and an oxygen atom. Besides, Pi-alkyl interactions were exhibited between Ala157, Leu183, Ala104, Leu207, Val91, Phe88 and benzene and furan rings. Likewise, a Pi-Pi-T-shaped bond was formed between the benzene ring and amino acid Ph288. Also, Pi-Sigma bonds were formed between Leu83 and the second benzene ring. Amino acids residues, namely Gly160, Tyr156, Glu155, Ala217, Lys106, Asp218, showed van der Waals interactions with carbon atoms C-3, C-4, C-7, C-9 and C-13. Besides, amino acids Tyr156, Gly160, Val91, Lys106, Asp218, Phe88, Ala217, Leu207, Leu83 formed hydrophobic interactions at the binding pocket (Table 4 and Figs 5, 7). Compound ZINC01404326 exhibited one hydrogen bond between the fluorine atom and amino acid Phe219. Likewise, Ala217, Leu83, Leu207 formed three Pi-Pi T-shaped bonds with two benzene ring2, seven Pi-alkyl bonds were formed between amino acids Phe88, Ala217, Ala157, Ala104, Leu83, Leu207 and three benzene rings and carbon atoms. Van der Waals interactions were formed between the amino acids Val91, Asp218, Leu138, Lys106, Glu155, Tyr156, Gly160 and carbon atoms C-4, C-6, C-7, C-11, C-12 and C-13, while hydrophobic interaction was shown with the amino acids Phe88, Glu204, Ala217, Val91, Gly160, Tyr165, Ala157, Leu207, Leu154, Phe219 (Table 4 and Figs 5, 7). Compound ZINC00882846 showed one hydrogen bond between the O atom and Phe219, while the other amino acids Glu155, Tyr156, Gly160, Lys106, Asp218, Ala217 formed van der Waals interactions with C-2, C-3, C-7, C-11, C-16 and C-17. Besides, hydrophobic interactions were formed between amino acids Leu83, Phe88,

Table 4. Details of binding interactions of the 6 compounds docked into binding pocket of Aurora kinase B

No	Ligands	Residue	Type of interactions
(1)	ZINC00190959	Phe219, Ala217, Try156, Lys106,	H-Bond
		Phe88, Ala218, Ala104, Leu138, Gly160, Pro158,	van der Waals
		Val91, Ala157, Leu83, Ala217,	Pi-Alky
		Lys106	Pi-cation
		Leu207, Leu83	Pi-Sigma
		Leu154, Val91, Gly160, Leu83, Leu207, Ohe88, Ala217	hydrophobic
(2)	ZINC07889110	Lys106, Phe219	H-Bond
		Leu138, Ala104, Tyr156, Gly160, Leu207, Ala217, Asp218	van der Waals
		Leu83, Val91	Pi-Alky
		Phe88	Pi-Pi-T-shaped
		Phe219	Pi-Sulfur
		Glu204, Phe88, Gly84, Val91, Leu83, Glu160, Ala217, Asp218	hydrophobic
(3)	ZINC00882851	Phe219	H-Bond
		Gly160, Tyr156, Glu155, Ala217, Lys106, Asp218	van der Waals
		Ala157, Leu183, Ala104, Leu207, Val91, Phe88,	Pi-Alky
		Phe288	Pi-Pi-T-shaped
		Leu83	Pi-Sigma
		Tyr156, Gly160, Val91, Lys106, Asp218,Phe88, Ala217, Leu207, Leu83	hydrophobic
(4)	ZINC01404326	Phe219	H-Bond
		Val91, Asp218, Leu138, Lys106, Glu155, Tyr156, Gly160	van der Waals
		Phe88, Ala217, Ala157, Ala104, Leu, 83, Leu207	Pi-Alky
		Ala217, Leu83, Leu207	Pi-Pi-T-shaped
		Ala217, Leu83, Leu207	Pi-Sigma
		Phe88, Glu204, Ala217, Val91, Gly160, Tyr165, Ala157, Leu207, Leu154, Phe219,	hydrophobic
(5)	ZINC00882846	Phe219	H-Bond
		Glu155, Tyr156, Gly160, Lys106, Asp218, Ala217	van der Waals
		Val91, Ala104, Leu138, Leu207, Ala157	Pi-Alky
		Phe88	Pi-Pi-T-shaped
		Leu83	Pi-Sigma
		Leu83, Phe88, Ala217, Val91, Gly160, Tyr156,	hydrophobic
(6)	ZINC08813187	Ala157	H-Bond
		Tyr156, Glu155, Leu138, Phe219, Val91, Gly160	van der Waals
		Phe88, Ala104, Leu207, Ala157	Pi-Alky
		Lys106	Pi-cation
		Ala217	Pi-Sigma
		Leu83, Leu207, Ala217	Pi-Pi-T-shaped
		Ala217, Phe219, Phe88, Leu83, Gly160, Leu2017, Tyr156, Leu154, Val91,	hydrophobic

Ala217, Val91, Gly160, Tyr156, and the C-1, C-2 C-3, C-7 C-8, C-14, C-15 and C-16 of the compound. Likewise, Gly118 showed hydrophobic interaction at the oxyanion hole. Pi-alkyl interactions were displayed between Val91, Ala104, Leu138, Leu207, Ala157 and benzene and furan rings. Besides, Pi-Sigma was noticed between Leu83 and the second benzene ring. Also, Phe88 formed a Pi-Pi-T-shaped bond with a benzene ring (Table 4 and Figs 5, 7).

Finally, Compound ZINC08813187 showed interactions similar to those displayed by the other compounds with the essential amino acids found in the binding pocket. Compound ZINC08813187 exhibited one hydrogen bond with the N atom. Likewise, Leu83, Leu207, Ala217 formed a Pi-Pi T-shaped bond with two benzene rings; besides, Pi-alkyl bonds were formed between amino acids Phe88, Ala104, Leu207, Ala157 and benzene ring. Another interaction was a van der Waals interaction formed between the amino acids residues Tyr156, Glu155, Leu138, Phe219, Val91, Gly160 and carbon atoms C-7, C-13, C-15, C-16, C-20, C-21 and C-22. Likewise, the compound exhibited hydrophobic interaction between the amino acids Ala217, Phe219, Phe88, Leu83, Gly160, Leu2017, Tyr156, Leu154, Val91 at the binding pocket (Table 4 and Figs 5,

7). The Ligplot+ program was used to show the interaction in 2D structure and to check the interactions obtained. The plot confirmed that all potential ligands interacted with the essential amino acid residues in the binding pocket (Fig. 7).

Molecular docking was performed between the target protein (PDB: 4AF3) and known Aurora Kinase inhibitors A, B, and C, namely CYC-116, PHA-739358, PHA-680632, AT9283, and ENMD-2076 (Borah and Reddy 2021). These compounds exhibited binding energy -9.2, -8.9, -8.8, -8.8 and -8.5, respectively. They interacted with the important amino acids in the binding pocket, such as Phe219, VAl91, Lys106, Leu154, Leu83, Gly160, Leu107, Ala207 and Phe88 with different interactions, such as H-bond, hydrophobic interactions, Pi-alky, and van der Waals interactions (Fig. 7). Even though these all the above compounds interacted at the binding pocket, our six potential compounds still show an advantage compared to the known drugs in terms of FEB and types of interactions that make them potential for Aurora Kinase inhibition. For the comparison, molecular docking against PDB: 4AF3 was performed on five compounds current in clinical trials as Aurora Kinase inhibitors: CYC-116, PHA-739358, PHA-680632, AT9283, and ENMD-2076.The docking results re-

Figure 7. Ligplot+ results of schematic ligand interactions of the 6 candidates showing hydrogen-bond and hydrophobic interactions (**A**) ZINC00190959, (**B**) ZINC07889110, (**C**) ZINC00882851, (**D**) ZINC01404326, (**E**) ZINC00882846, (**F**) ZINC08813187.

Figure 8. 3D structure of five clinical trial compounds used as Kinase AURK (A, B and C), namely CYC-116, PHA-739358, PHA-680632, AT9283 and ENMD-2076 in the binding pocket of (PDB:4AF3).

vealed a variety of possible interactions between the amino acids in the binding pocket. Among the inhibitors was compound CYC-116, which showed the FEB of −8.7 kcal/mol, and few interactions with the amino acids, one hydrogen bond with Pha219, one van deer Waals with Gly169; Pi-Pi T-shaped interaction was formed with Leu83, Leu207, and Ala217. Besides, Pi-alkyl bonds were formed with amino acids Phe88, Ala104, Leu207, and Ala157 (Fig. 8).

Compound PHA-739358 exhibiting FEB of −7.5 kcal/mol was found to show four types of interactions. Three van deer Waals interactions with Gly84, Gly160 and Pro158, Pi-alkyl with Lys106, Val91, Leu154, and Ala117. In addition, PHA-739358 displayed one hydrogen bond with amino acid Glu161, and one Pi-sigma with Leu83 (Fig. 8). Similar to the other inhibitors, PHA-680632 exhibited FEB of −7.5 kcal/mol with four types of interactions: one Pi-sigma bond with Phe88, van deer Waals also displayed with Pha219, Leu154, Arg81, Gly160 and Pro158. Besides five Pi-alkyl bonds were formed with Ala217, Val91, Leu207, Leu83 and Arg159 (Fig. 8). Compound AT9283 exhibited FEB of −7.5 kcal/mol with five types of interaction. AT9283 exhibited one hydrogen bond with Ala217, three van der Waals interactions formed with Leu154, Pha219 and Gly84; a carbon hydrogen bond was formed with amino acids Gly180 and Gly161. In addition Pi-Pi-stacked bonds with Phe88, and three Pi-alkyl bonds were formed with Val91, Leu83 and Leu207; besides, Pi-Cation bond was formed with Lys106 (Fig. 8). Compound ENMD-2076 exhibiting FEB of −7.5 kcal/mol was found to show two van der Waals interactions with Arg159, Arg81 and Val19 and one Pi-Cation with Glu161. Pi-alkyl bond was formed with Leu83 and Pi-sigma with Leu207 (Fig. 8).

A careful analysis of the docking scores of our compounds compared to the co-crystallized ligand VX-680 in the human Aurora B kinase revealed that the docking scores of our compounds were better than those of VX-680. Furthermore, a detailed analysis of all hydrogen bonds produced by these ligands with the protein exhibited a similar binding site to VX-680 (ALA157, GLU155 and LEU207). The above finding confirmed hat good interaction with high affinity and low FEB was shown by the six identified compounds from the ZINC database. The ability of these compounds to interact with the essential amino acid restudies in the binding pocket could be used to enhance the selectivity of the chose compounds to Aurora B kinase, suggesting extra benefits of inhibiting the target protein. Furthermore, the identified compounds show an advantage over the current compound drug in the clinical trial stage in terms of the FEB, the pattern of interaction, and the amount of interaction with essential amino acids in the binding pocket, making them the potential for Aurora Kinase B inhibitors.

Conclusion

The current research successfully applied virtual screening, molecular docking and interaction analysis to identify six potent inhibitors for Aurora Kinase B. The six compounds were ZINC00190959, ZINC07889110, ZINC0088285, ZINC01404326, ZINC00882846 and ZINC08813187, which showed lower FEB against the target protein binding pocket. The FEB were as follows -11.92, -11.85, -11.46, -11.33, -11.21 and -11.1 kcal/mol for AutoDock and -11.7, -11.5, -11.2, -11.0, -10.8 and -10.6 kcal/mol for AutoDock Vina, respectively. The results indicate that the six compounds bonded strongly to the active pocket of Aurora Kinase B in comparison to the current approved clinical trial drugs. Additionally, because the top six docking hits pass the Lipinski rule of five, they are likely to be orally active drugs. The findings demonstrated that the compounds' interactions with the essential amino acids were closer than the coordinated ligand VX-680 and the current clinical trial drug. Further studies into the effects of the compounds on Aurora kinase B using experimental investigations (in vitro) and an appropriate animal model are needed to confirm this finding.

Conflict of interests

The authors declare no conflict of interests.

References

- Abagyan R, Totrov M (2001) High-throughput docking for lead generation. Current Opinion in Chemical Biology 5(4): 375–382. https://doi.org/10.1016/S1367-5931(00)00217-9 [PubMed]
- Abdalsalam AAA (2017) *In-silico* virtual screening and ADMET study to find novel neuraminidase N1 inhibitors extended to the 150-cavity. Journal of Applied Pharmaceutical Science 7(5): 024–033. https://doi.org/10.7324/JAPS.2017.70505
- Abdusalam AAA, Vikneswaran M (2020) Novel acetylcholinesterase inhibitors identified from zinc database using docking-based virtual screening for Alzheimer's disease. ChemistrySelect 5(12): 3593–3599. https://doi.org/10.1002/slct.201904177
- Ahmed A, Shamsi A, Mohammad T, Hasan GM, Islam A, Hassan M (2021) Aurora B kinase: A potential drug target for cancer therapy. Journal of Cancer Research and Clinical Oncology 147(8): 2187–2198. https://doi.org/10.1007/s00432-021-03669-5 [PubMed]
- Al-Warhi T, Sabt A, Elkaeed EB, Eldehna WM (2020) Recent advancements of coumarin-based anticancer agents: An up-to-date review. Bioorganic Chemistry 103 104163. https://doi.org/10.1016/j.bioorg.2020.104163 [PubMed]
- Balamurugan R, Stalin A, Ignacimuthu S (2012) Molecular docking of γ-sitosterol with some targets related to diabetes. European Journal of Medicinal Chemistry 47(1): 38–43. https://doi.org/10.1016/j.ejmech.2011.10.007 [PubMed]
- Bhullar KS, Lagarón NO, McGowan EM, Parmar I, Jha A, Hubbard BP, Rupasinghe HP (2018) Kinase-targeted cancer therapies: progress, challenges and future directions. Molecular Cancer 17(1): 1–20. https://doi.org/10.1186/s12943-018-0804-2 [PubMed] [PMC]
- Borah NA, Reddy MM (2021) Aurora kinase B inhibition: a potential therapeutic strategy for cancer. Molecules 26(7): 1981. https://doi.org/10.3390/molecules26071981 [PubMed] [PMC]
- Bourne Y, Taylor P, Radić Z, Marchot P (2003) Structural insights into ligand interactions at the acetylcholinesterase peripheral anionic site. The EMBO Journal 22(1): 1–12. https://doi.org/10.1093/emboj/cdg005 [PubMed] [PMC]

- Bourzikat O, El Abbouchi A, Ghammaz H, El Brahmi N, El Fahime E, Paris A, Daniellou R, Suzenet F, Guillaumet G, El Kazzouli S (2022) Synthesis, anticancer activities and molecular docking studies of a novel class of 2-phenyl-5, 6, 7, 8-tetrahydroimidazo [1, 2-b] pyridazine derivatives bearing sulfonamides. Molecules 27(16): 5238. https://doi.org/10.3390/molecules27165238 [PubMed] [PMC]

- Brognard J, Hunter T (2011) Protein kinase signaling networks in cancer. Current Opinion in Genetics & Development 21(1): 4–11. https://doi.org/10.1016/j.gde.2010.10.012 [PubMed] [PMC]

- Carlsson J, Yoo L, Gao ZG, Irwin JJ, Shoichet BK, Jacobson KA (2010) Structure-based discovery of A2A adenosine receptor ligands. Journal of Medicinal Chemistry 53(9): 3748–3755. https://doi.org/10.1021/jm100240h [PubMed] [PMC]

- Carmena M, Earnshaw WC (2003) The cellular geography of aurora kinases. Nature Reviews Molecular Cell Biology 4(11): 842–854. https://doi.org/10.1038/nrm1245 [PubMed]

- Cavasotto CN, Adler NS, Aucar MG (2018) Quantum chemical approaches in structure-based virtual screening and lead optimization. Frontiers in Chemistry 6: 188. https://doi.org/10.3389/fchem.2018.00188 [PubMed] [PMC]

- Chan KS, Koh CG, Li HY (2012) Mitosis-targeted anti-cancer therapies: where they stand. Cell Death & Disease 3(10): e411. https://doi.org/10.1038/cddis.2012.148 [PubMed] [PMC]

- Chohan TA, Qayyum A, Rehman K, Tariq M, Akash MS (2018) An insight into the emerging role of cyclin-dependent kinase inhibitors as potential therapeutic agents for the treatment of advanced cancers. Biomedicine & Pharmacotherapy 107: 1326–1341. https://doi.org/10.1016/j.biopha.2018.08.116 [PubMed]

- Cordeiro MN, Speck-Planche A (2012) Computer-aided drug design, synthesis and evaluation of new anti-cancer drugs. Current Topics in Medicinal Chemistry 12(24): 2703–2704. https://doi.org/10.2174/1568026611212240001 [PubMed] [PMC]

- Dai J, Dan W, Li N, Wang J (2018) Computer-aided drug discovery: Novel 3, 9-disubstituted eudistomin U derivatives as potent antibacterial agents. European Journal of Medicinal Chemistry 157: 333–338. https://doi.org/10.1016/j.ejmech.2018.08.001 [PubMed]

- Duan H, Liu X, Zhuo W, Meng J, Gu J, Sun X, Zuo K, Luo Q, Luo Y, Tang D, Shi H (2019) 3D-QSAR and molecular recognition of Klebsiella pneumoniae NDM-1 inhibitors. Molecular Simulation 45(9): 694–705. https://doi.org/10.1080/08927022.2019.1579327

- Elkins JM, Santaguida S, Musacchio A, Knapp S (2012) Crystal structure of human aurora B in complex with INCENP and VX-680. Journal of Medicinal Chemistry 55(17): 7841–7848. https://doi.org/10.1021/jm3008954 [PubMed] [PMC]

- Failes TW, Mitic G, Abdel-Halim H, Po'Uha ST, Liu M, Hibbs DE, Kavallaris M (2012) Evolution of resistance to Aurora kinase B inhibitors in leukaemia cells. PLoS ONE 7(2): e30734. https://doi.org/10.1038/sj.bjp.0707305 [PubMed] [PMC]

- Fodero LR, Mok SS, Losic D, Martin LL, Aguilar MI, Barrow CJ, Livett BG, Small DH (2004) α7-Nicotinic acetylcholine receptors mediate an Aβ1− 42-induced increase in the level of acetylcholinesterase in primary cortical neurones. Journal of Neurochemistry 88(5): 1186–1193. https://doi.org/10.1046/j.1471-4159.2003.02296.x [PubMed]

- Fulcher LJ, Sapkota GP (2020) Mitotic kinase anchoring proteins: the navigators of cell division. Cell Cycle 19(5): 505–524. https://doi.org/10.1080/15384101.2020.1728014 [PubMed] [PMC]

- Horvath D (1997) A virtual screening approach applied to the search for trypanothione reductase inhibitors. Journal of Medicinal Chemistry 40(15): 2412–2423. https://doi.org/10.1021/jm9603781 [PubMed]

- Irwin JJ, Shoichet BK (2005) ZINC − a free database of commercially available compounds for virtual screening. Journal of Chemical Information and Modeling 45(1): 177–182. https://doi.org/10.1021/ci049714 [PubMed] [PMC]

- Irwin JJ, Sterling T, Mysinger MM, Bolstad ES, Coleman RG (2012) ZINC: a free tool to discover chemistry for biology. Journal of Chemical Information and Modeling 52(7): 1757–1768. https://doi.org/10.1021/ci3001277 [PubMed] [PMC]

- Kuang X, Li J (2022) Chromosome instability and aneuploidy as context-dependent activators or inhibitors of antitumor immunity. Frontiers in Immunology 13: 895961. https://doi.org/10.3389/fimmu.2022.895961 [PubMed] [PMC]

- Laskowski RA, Swindells MB (2011). LigPlot+: multiple ligand–protein interaction diagrams for drug discovery. Journal of Chemical Information and Modeling 51(10): 2778–2786. https://doi.org/10.1021/ci200227u [PubMed]

- Lin ZZ, Chou CH, Cheng AL, Liu WL, Chia-Hsien Cheng J (2014) Radiosensitization by combining an aurora kinase inhibitor with radiotherapy in hepatocellular carcinoma through cell cycle interruption. International Journal of Cancer 135(2): 492–501. https://doi.org/10.1002/ijc.28682 [PubMed]

- Lipinski CA (2004) Lead-and drug-like compounds: the rule-of-five revolution. Drug Discovery Today. Technologies 1(4): 337–341. https://doi.org/10.1016/j.ddtec.2004.11.007 [PubMed]

- Liu T, Lin Y, Wen X, Jorissen RN, Gilson MK (2007) BindingDB: a web-accessible database of experimentally determined protein-ligand binding affinities. Nucleic Acids Research 35(suppl_1): D198–D201. https://doi.org/10.1093/nar/gkl999 [PubMed] [PMC]

- Lohning A, Levonis SM, Williams-Noonan B, Schweiker SS (2017) A practical guide to molecular docking and homology modelling for medicinal chemists. Current Topics in Medicinal Chemistry 17(18): 2023–2040. https://doi.org/10.2174/1568026617666170130110827 [PubMed]

- Martin EJ, Jansen JM (2020) Biased diversity for effective virtual screening. Journal of Chemical Information and Modeling 60(9): 4116–4119. https://doi.org/10.1021/acs.jcim.9b01155 [PubMed]

- Mbemi A, Khanna S, Njiki S, Yedjou CG, Tchounwou PB (2020) Impact of gene–environment interactions on cancer development. International Journal of Environmental Research and Public Health 17(21): 8089. https://doi.org/10.3390/ijerph17218089 [PubMed] [PMC]

- Mysinger MM, Shoichet BK (2010) Rapid context-dependent ligand desolvation in molecular docking. Journal of Chemical Information and Modeling 50(9): 1561–1573. https://doi.org/10.1021/ci100214a [PubMed]

- Negrini S, Gorgoulis VG, Halazonetis TD (2010) Genomic instability-an evolving hallmark of cancer. Nature Reviews. Molecular Cell Biology 11(3): 220–228. https://doi.org/10.1038/nrm2858 [PubMed]

- Phatak SS, Stephan CC, Cavasotto CN (2009) High-throughput and in silico screenings in drug discovery. Expert Opinion on Drug Discovery 4(9): 947–959. https://doi.org/10.1517/17460440903190961 [PubMed]

- Shaker B, Ahmad S, Lee J, Jung C, Na D (2021) *In silico* methods and tools for drug discovery. Computers in Biology and Medicine 137: 104851. https://doi.org/10.1016/j.compbiomed.2021.104851 [PubMed]

- Shen Z (2011) Genomic instability and cancer: an introduction. Journal of Molecular Cell Biology 3(1): 1–3. https://doi.org/10.1093/jmcb/mjq057 [PubMed]

- Shoichet BK (2004) Virtual screening of chemical libraries. Nature 432(7019): 862–865. https://doi.org/10.1038/nature03197
- Smith DM, Daniel KG, Wang Z, Guida WC, Chan TH, Dou QP (2004) Docking studies and model development of tea polyphenol proteasome inhibitors: applications to rational drug design. Proteins: Structure, Function, and Bioinformatics 54(1): 58–70. https://doi.org/10.1002/prot.10504 [PubMed]
- Sousa SF, Ribeiro AJ, Coimbra JT, Neves RP, Martins SA, Moorthy NS, Fernandes PA, Ramos MJ (2013) Protein-ligand docking in the new millennium–a retrospective of 10 years in the field. Current Medicinal Chemistry 20(18): 2296–2314. https://doi.org/10.2174/0929867311320180002 [PubMed]
- Stumpfe D, Bajorath J (2020) Current trends, overlooked issues, and unmet challenges in virtual screening. Journal of Chemical Information and Modeling 60(9): 4112–4115. https://doi.org/10.1021/acs.jcim.9b01101 [PubMed]
- Takeshima H, Ushijima T (2019) Accumulation of genetic and epigenetic alterations in normal cells and cancer risk. NPJ Precision Oncology 3(1): 1–8. https://doi.org/10.1038/s41698-019-0079-0 [PubMed] [PMC]
- Taylor RD, Jewsbury PJ, Essex JW (2002) A review of protein-small molecule docking methods. Journal of Computer-aided Molecular Design 16(3): 151–166. https://doi.org/10.1023/A:1020155510718 [PubMed]
- ur Rashid H, Xu Y, Muhammad Y, Wang L, Jiang J (2009) Research advances on anticancer activities of matrine and its derivatives: an updated overview. European Journal of Medicinal Chemistry 161: 205–238. https://doi.org/10.1016/j.ejmech.2018.10.037 [PubMed]
- Velmurugan D, Pachaiappan R, Ramakrishnan C (2020) Recent trends in drug design and discovery. Current Topics in Medicinal Chemistry 20(19): 1761–1770. https://doi.org/10.2174/1568026620666200622150003 [PubMed]
- Welburn JP, Jeyaprakash AA (2018) Mechanisms of mitotic kinase regulation: a structural perspective. Frontiers in Cell and Developmental Biology 6: 6. https://doi.org/10.3389/fcell.2018.00006 [PubMed] [PMC]
- Willems E, Dedobbeleer M, Digregorio M, Lombard A, Lumapat PN, Rogister B (2018) The functional diversity of Aurora kinases: a comprehensive review. Cell Division 13(1): 1–7. https://doi.org/10.1186/s13008-018-0040-6 [PubMed] [PMC]
- Yamashita S, Kishino T, Takahashi T, Shimazu T, Charvat H, Kakugawa Y, Nakajima T, Lee YC, Iida N, Maeda M, Hattori N (2018) Genetic and epigenetic alterations in normal tissues have differential impacts on cancer risk among tissues. Proceedings of the National Academy of Sciences 115(6): 1328–1333. https://doi.org/10.1186/s13148-019-0789-8 [PubMed] [PMC]
- Zoete V, Cuendet MA, Grosdidier A, Michielin O (2011) SwissParam: a fast force field generation tool for small organic molecules. Journal of Computational Chemistry 32(11): 2359–2368. https://doi.org/10.1002/jcc.21816 [PubMed]

Author contribution

- **Ashraf Ahmed Ali Abdusalam**, PhD, Assistant Professor, Head of the Department of Pharmaceutical Sciences, Faculty of Health Science, e-mail: aalmansory@su.edu.ly, ORCID ID https://orcid.org/0000-0002-3309-1207. The author was only the contributor of the article.